PTA/PTA/06-48
hep-ph/0610085
October 2006
Revised version

A FORTRAN code for $\gamma\gamma \to ZZ$ in SM and MSSM†

Th. Diakonidis[a], G.J. Gounaris[a] and J. Layssac[b]

[a]Department of Theoretical Physics, Aristotle University of Thessaloniki,
Gr-54006, Thessaloniki, Greece.

[b]Laboratoire de Physique Théorique et Astroparticules, UMR 5207,
Université Montpellier II, F-34095 Montpellier Cedex 5.

Abstract

Through the present paper, the code **gamgamZZ** is presented, which may be used to calculate all possible observables related to the process $\gamma\gamma \to ZZ$, in either the Standard Model (SM), or the minimal sypersymmetric standard model (MSSM) with real parameters.

†Work co-funded by the European Union - European Social fund and the National fund PYTHAGORAS EPEAEK II

1 Introduction

The starting of the LHC operation in 2007 brings closer the moment where we will be able to see whether the simplest Standard Model (SM) higgs particle really exists [1], and whether the much searched for scale of New Physics (NP) lies in the TeV range [2].

Among the many such NP forms, the most widely studied is certainly $\mathcal{N} = 1$ Supersymmetry (SUSY) in four dimensions. Hints supporting the minimal supersymmetric model (MSSM), with real electroweak scale parameters, are supplied by the unification of the gauge couplings at the scale of $\sim 2 \cdot 10^{16}$ GeV and the proximity of this scale to the one needed for understanding the neutrino masses and leptogenesis [3]. The easy accommodation of Dark Matter in R-parity conserving SUSY models, is also encouraging.

But, if SUSY candidates are discovered at LHC [4, 5, 6], the need to check in detail their properties in an international linear collider (ILC) will be overwhelming [7, 8, 9].

This note concerns the important option of ILC to run as a $\gamma\gamma$ collider $ILC_{\gamma\gamma}$, using back scattering of $e^{\pm}$-beams by laser photons [10, 11, 12]. In many instances, such a $\gamma\gamma$ collider is more efficient for studying new physics, than the standard e^-e^+-ILC [13, 14, 15, 16].

A very important set of processes observable in $ILC_{\gamma\gamma}$, consists of the neutral gauge boson production

$$\gamma\gamma \to \gamma\gamma, \ \gamma Z, \ ZZ \quad , \tag{1}$$

which are first realized at the 1-loop level, in both SM and MSSM, and could therefore be very sensitive to possible new physics. Their analytical 1-loop study was first performed for SM in [17, 18, 19], and subsequently extended to include all possible MSSM contributions, with real μ and soft SUSY parameters [20, 21, 22, 23].

It has been found there that, at c.m. energies above 200GeV, the dominant helicity amplitudes for the processes (1) are mostly imaginary and satisfy helicity conservation (HC), which forces the sum of the helicities of the two incoming photons to be equal to the sum of the helicities of the two outgoing gauge bosons [24]. This striking phenomenon mainly comes from the W-loop, and could make these processes a very interesting field of study in $ILC_{\gamma\gamma}$. Thus, if *e.g.* SUSY candidates are discovered at LHC, the study of (1) at the contemplated 1% level of accuracy, should provide important checks of their nature.

In studying (1), the independent helicity amplitudes have been expressed in terms of the simplest Veltman-Passarino functions B_0, C_0, D_0 [25]. The resulting formulae are quite manageable for the $\gamma\gamma$ and γZ cases. For $\gamma\gamma \to ZZ$ though, the analytic expressions of [22, 23], particularly for MSSM, are so complicated, that a public numerical code will be very useful.

The purpose of the present paper is to release such code "gamgamZZ", applying to SM and MSSM, for any set of real parameters [26]. For both models, the code calculates the independent helicity amplitudes for $\gamma\gamma \to ZZ$, as well as the observable cross sections in $LC_{\gamma\gamma}$, for the case where the polarizations of the final ZZ-pair are summed over. The definitions of these amplitudes and cross sections are given in Section 2. In Section 3, we discuss the code and give some numerical examples. Section 4 contains the Conclusions.

2 The $\gamma\gamma \to ZZ$ helicity amplitudes and cross sections

We are interested in the process

$$\gamma(p_1,\lambda_1)\gamma(p_2,\lambda_2) \to Z(p_3,\lambda_3)Z(p_4,\lambda_4) \ \ , \tag{2}$$

where the momenta p_j and helicities λ_j, of the incoming and outgoing particles are indicated in parentheses. The generic form of the relevant 1-loop Feynman diagrams is indicated in Fig.1a,b. The corresponding helicity amplitudes, denoted as[1] $F_{\lambda_1\lambda_2\lambda_3\lambda_4}(\beta_Z,t,u)$, are expressed in terns of the kinematical variables

$$s \equiv s_{\gamma\gamma} = (p_1+p_2)^2 = \frac{4m_Z^2}{1-\beta_Z^2} \ \ , \tag{3}$$

$$t = (p_1-p_3)^2 = m_Z^2 - \frac{s}{2}(1-\beta_Z\cos\theta) \ \ , \tag{4}$$

$$u = (p_1-p_4)^2 = m_Z^2 - \frac{s}{2}(1+\beta_Z\cos\theta) \ , \tag{5}$$

where θ is the c.m scattering angle, and β_Z coincides with the Z-velocity in the ZZ c.m. frame, provided its positive sign is selected from (3). The possible values of (λ_1,λ_2) are ±1; while those of (λ_3,λ_4) are$(\pm1,0)$.

Bose statistics, combined with the Jacob-Wick (JW) phase conventions [27], demand

$$F_{\lambda_1\lambda_2\lambda_3\lambda_4}(\beta_Z,t,u) = F_{\lambda_2\lambda_1\lambda_4\lambda_3}(\beta_Z,t,u)(-1)^{\lambda_3-\lambda_4} \ , \tag{6}$$

$$F_{\lambda_1\lambda_2\lambda_3\lambda_4}(\beta_Z,t,u) = F_{\lambda_2\lambda_1\lambda_3\lambda_4}(\beta_Z,u,t)(-1)^{\lambda_3-\lambda_4} \ , \tag{7}$$

$$F_{\lambda_1\lambda_2\lambda_3\lambda_4}(\beta_Z,t,u) = F_{\lambda_1\lambda_2\lambda_4\lambda_3}(\beta_Z,u,t) \ , \tag{8}$$

while CP invariance implies

$$F_{\lambda_1\lambda_2\lambda_3\lambda_4}(\beta_Z,t,u) = F_{-\lambda_1,-\lambda_2,-\lambda_3,-\lambda_4}(\beta_Z,t,u)(-1)^{\lambda_3-\lambda_4} \ . \tag{9}$$

These relations allow the calculation of the complete set of the 36 helicity amplitudes, in terms of the 10 basic ones

$$\begin{aligned} &F_{+++-}(\beta_Z,t,u) \ , \ F_{++++}(\beta_Z,t,u), \\ &F_{+-++}(\beta_Z,t,u) \ , \ F_{+-00}(\beta_Z,t,u) \ , \\ &F_{++00}(\beta_Z,t,u) \ , \ F_{+++0}(\beta_Z,t,u), \\ &F_{+-+0}(\beta_Z,t,u) \ , \ F_{+-+-}(\beta_Z,t,u) \ , \\ &F_{++--}(\beta_Z,t,u) \ , \ F_{++-0}(\beta_Z,t,u) \ . \end{aligned} \tag{10}$$

In [22, 23] these amplitudes have been analytically expressed in terms of the $B_0,\ C_0,\ D_0$ Passarino-Veltman [25] functions. The code presented bellow is based on these expressions. As far as SM is concerned, these results agree with those of [19], except for a trivial

[1] Their sign is related to the sign of the S-matrix through $S_{\lambda_1\lambda_2\lambda_3\lambda_4} = 1 + i(2\pi)^4\delta(p_4+p_3-p_1-p_2)F_{\lambda_1\lambda_2\lambda_3\lambda_4}$.

misprint in F_{+-+0}, pointed out in [23].

As expected on the basis of the helicity conservation (HC) theorem, established in [24] for any two body process, the dominant helicity amplitudes in either SM or MSSM, should obey

$$\lambda_1 + \lambda_2 = \lambda_3 + \lambda_4 \quad , \tag{11}$$

for s and $|t|$ much larger than all squared masses in the model. In MSSM, HC is an exact asymptotic theorem; while in SM, it has only been proven to 1-loop leading logarithmic accuracy [24].

This means that, at asymptotic energies and finite angles, all MSSM amplitudes of the set (10) should vanish, except (F_{++++}, F_{+-+-}, F_{+-00}), which increase logarithmically with energy and are mostly imaginary [22] .

We have checked numerically that the 1-loop results of [22, 23], indeed obey this rule. This is particularly striking for F_{++00}, where various contributions, often involving ratios of gauge, chargino and charged higgs masses, have been seen to cancel each other exactly at asymptotic $s, |t|$. The validity of HC provides a very nice check of our code.

HC is essentially true also for SM, the only difference being that the amplitudes that violate (11) go asymptotically to small generally non-vanishing constants.

Backscattering polarized laser photons off polarized $e^{\mp}$-beams, would realize an $ILC_{\gamma\gamma}$ collider [10, 12]. Restricting to the case that the final Z polarizations are not studied, the observable cross sections at $ILC_{\gamma\gamma}$ are given by [22, 23]

$$\frac{d\sigma_0(\gamma\gamma \to ZZ)}{d\cos\theta} = \left(\frac{\beta_Z}{128\pi\hat{s}}\right) \sum_{\lambda_3\lambda_4} [|F_{++\lambda_3\lambda_4}|^2 + |F_{+-\lambda_3\lambda_4}|^2] \ , \tag{12}$$

$$\frac{d\sigma_{22}(\gamma\gamma \to ZZ)}{d\cos\theta} = \left(\frac{\beta_Z}{128\pi\hat{s}}\right) \sum_{\lambda_3\lambda_4} [|F_{++\lambda_3\lambda_4}|^2 - |F_{+-\lambda_3\lambda_4}|^2] \ , \tag{13}$$

$$\frac{d\sigma_3(\gamma\gamma \to ZZ)}{d\cos\theta} = \left(\frac{-\beta_Z}{64\pi\hat{s}}\right) \sum_{\lambda_3\lambda_4} Re[F_{++\lambda_3\lambda_4} F^*_{-+\lambda_3\lambda_4}] \ , \tag{14}$$

$$\frac{d\sigma_{33}(\gamma\gamma \to ZZ)}{d\cos\theta} = \left(\frac{\beta_Z}{128\pi\hat{s}}\right) \sum_{\lambda_3\lambda_4} Re[F_{+-\lambda_3\lambda_4} F^*_{-+\lambda_3\lambda_4}] \ , \tag{15}$$

$$\frac{d\sigma'_{33}(\gamma\gamma \to ZZ)}{d\cos\theta} = \left(\frac{\beta_Z}{128\pi\hat{s}}\right) \sum_{\lambda_3\lambda_4} Re[F_{++\lambda_3\lambda_4} F^*_{--\lambda_3\lambda_4}] \ , \tag{16}$$

$$\frac{d\sigma_{23}(\gamma\gamma \to ZZ)}{d\cos\theta} = \left(\frac{\beta_Z}{64\pi\hat{s}}\right) \sum_{\lambda_3\lambda_4} Im[F_{++\lambda_3\lambda_4} F^*_{+-\lambda_3\lambda_4}] \ , \tag{17}$$

in terms of the helicity amplitudes satisfying (6-10).

3 The gamgamZZ code

The released code gamgamZZ.tar.gz [26], consists of four FORTRAN codes. Two of them, **sm1_1** and **mssm1_1**, calculate the 10 basic $\gamma\gamma \to ZZ$ helicity amplitudes (10), in SM and MSSM respectively. The remaining helicity amplitudes may then be obtained using (6-9). The needed higgs width may be calculated from *e.g.* [28].

For compiling these codes, LoopTools [29] is required. All input parameters are contained in input files called "susypar.in" in both, the SM and the MSSM case. All dimensional parameters are in TeV. The results for each $\gamma\gamma$ c.m. energy, are given for $N_\theta + 1$ equal steps of $\cos\theta$, starting from $\cos(\theta_a)$ and ending in $\cos(\theta_b)$. The integer parameter N_θ, and the angles θ_a and θ_b in degrees, are specified in the in-file.

As an example we give in Table 1 the results of the **sm1_1** output, for 5 of the 10 helicity amplitudes listed in (10) and $N_\theta = 8$. A similar output is created for the remaining five basic amplitudes. The c.m. energy is taken at $\sqrt{s} = 0.5$TeV. The exact form of all outputs is explained in the Readme.dat file accompanying the codes.

Table 1: Form of the **sm1_1** output for 5 of the 10 helicity amplitudes listed in (10). A similar form appears in the same output for the description of the remaining five amplitudes of (10).

$\cos\theta$	ReF_{++++}	ImF_{++++}	ReF_{+-++}	ImF_{+-++}	ReF_{+-00}	ImF_{+-00}	ReF_{++00}	ImF_{++00}	ReF_{+++0}	ImF_{+++0}
0.866	0.144E-1	0.162	0.671E-3	0.179E-2	-0.328E-3	0.360E-2	-0.267E-2	-0.473E-2	0.551E-3	0.183E-2
0.707	0.104E-1	0.137	0.655E-3	0.204E-2	-0.561E-3	0.633E-2	-0.246E-2	-0.426E-2	0.351E-3	0.124E-2
0.500	0.772E-2	0.120	0.472E-3	0.228E-2	-0.832E-3	0.857E-2	-0.227E-2	-0.390E-2	0.164E-3	0.783E-3
0.259	0.631E-2	0.110	0.322E-3	0.244E-2	-0.104E-2	1.000E-2	-0.215E-2	-0.368E-2	0.594E-4	0.381E-3
0.0	0.588E-2	0.107	0.2679E-3	0.250E-2	-0.112E-2	0.105E-1	-0.211E-2	-0.361E-2	0.0	0.0
-0.259	0.631E-2	0.110	0.322E-3	0.244E-2	-0.104E-2	1.000E-2	-0.215E-2	-0.368E-2	-0.594E-4	-0.381E-3
-0.500	0.771E-2	0.120	0.472E-3	0.228E-2	-0.832E-3	0.857E-2	-0.227E-2	-0.390E-2	-0.164E-3	-0.783E-3
-0.707	0.104E-1	0.137	0.655E-3	0.204E-2	-0.561E-3	0.633E-2	-0.246E-2	-0.426E-2	-0.351E-3	-0.124E-2
-0.866	0.1443E-1	0.162	0.671E-3	0.179E-2	-0.328E-3	0.360E-2	-0.267E-2	-0.473E-2	-0.551E-3	-0.183E-2

The other two codes, **sm2** and **mssm2** are compiled similarly and calculate the differential cross sections (12-17) in SM and MSSM respectively. They follow a similar format, fully explained in the aforementioned Readme.dat file. These results do not of course include the $ILC_{\gamma\gamma}$luminosity functions. But it should be easy to combine them with a code like CompAZ in order to calculate ZZ production in a realistic $ILC_{\gamma\gamma}$ environment [31].

The **sm1_1**, **sm2** codes give the exact SM 1-loop contribution from the diagrams in Fig.1a,b.

Correspondingly, the MSSM codes **mssm1_1**, **mssm2** contain the exact W, higgs, quark and lepton loop contributions due to the box and triangular diagrams in Fig.1a,b. The sfermion and chargino 1-loop triangular contributions from the diagrams[2] in Fig.1b are also calculated exactly.

In these codes though, we have neglected the sfermion and chargino mixing effects, arising from the non-diagonal Z couplings, in the box diagrams of Fig.1a. This is always a very good approximation for the (very small) sfermion box contribution. It is

[2]The chargino or sfermion mixing cannot induce a non-diagonal Z-coupling contribution in this case.

also true for the chargino box contribution for all helicity amplitudes, except for the amplitudes involving two longitudinal Z bosons. The reason for this is because the high energy chargino-box contribution to the production of a longitudinal gauge boson is determined by the gaugino-higgsino-higgs coupling [30], for which chargino mixing cannot be neglected. The only amplitudes of (10) belonging to this category are F_{++00} and F_{+-00}, for which the chargino box contribution is approximated by the asymptotic part of (A.37, A.38) of [22] and (A.57, A.58, A.63, A.64) of [23]. This is an adequate approximation, since these contributions are rather energy independent and very small.

If it becomes necessary, the exact chargino 1-loop box contribution could be included in our codes, by using the full analytical expressions appearing in (A.36-A.66) of the Appendix of [23].

It is also important to note that when using LoopTools [29] for calculating the needed Passarino-Veltman functions, problems may appear related to the small masses of the quarks and leptons of the first two families. We have checked that if the LoopTools1.2 version is used, there is no difficulty. For LoopTools2 and newer versions though, the masses of the quarks and charge leptons of the first two families should be increased to around 7 or 8 MeV, to overcome this problem. This does not reduce the accuracy of our results, and is easily done by changing the input parameters in the in-file.

As an example, we present in Figs.2-4 the differential and integrated cross sections σ_0 and σ_{22}, defined in (12, 13), for SM (with $m_H = 130$GeV) and for the two benchmark MSSM models $SPS1a'$ [5] and "light higgs" [6]. $SPS1a'$ is an mSUGRA model with ($m_0 = 70$ GeV, $m_{1/2} = 250$ GeV, $A_0 = -300$ GeV, $\tan\beta = 10$); while in "light higgs", the electroweak scale parameters have been selected as $M_1 = 150$GeV, $M_2 = 300$GeV, $M_3 = 600$GeV, $A_t = A_b = A_\tau = 700$GeV, $\mu = 700$GeV, $m_{A^0} = 104$ GeV, $\tan\beta = 34.4$ and all sfermion masses are set at 340GeV [6]. In all cases, the top mass was put at $m_t = 173.8$GeV.

The specific cross sections $\sigma_0,\ \sigma_{22}$ have been chosen because they often give the largest effect. They are also the ones that receive contributions from the s-channel[3] higgs exchange diagrams of Fig.1b. Thus, if the SM higgs is above the ZZ-threshold but not too heavy, a higgs peak should be visible in the σ_0 and σ_{22}-plots [23]. This applies also to MSSM, provided that the heavier neutral higgs particle H^0 is above the ZZ-threshold and its couplings are appropriate; see examples in [23]. Among the scenarios considered here though, only $SPS1a'$, implying $m_{H^0} = 0.424$TeV, satisfies the $2m_Z$ constraint. But the H^0 contribution is so weak in this model, that no peak is visible in Figs.4.

In any case, the SUSY modifications to the SM predictions for σ_0 and σ_{22}, are generally energy dependent and sometimes considerably larger than 1%. Therefore, SUSY effects in an $ILC_{\gamma\gamma}$ study of $\gamma\gamma \to ZZ$, may be observable and useful.

Before finishing this Section, it is important to remember that nowadays, and surely

[3] In fact the only cross sections that receive such contributions are $\sigma_0,\ \sigma_{22},\ \sigma_{23}$; compare (12-17).

much more in the future, computer codes like FORMCALC [32] or GRACE-LOOP [33] are being developed which, starting from a given Lagrangian, construct automatically all vertices[4], draw the necessary diagrams and calculate all amplitudes in an analytic (or semi-analytic) way. Applying to $\gamma\gamma \to ZZ$, this means that all work contained in *e.g.* [22, 23] is done in an automatic way, obviously deriving similar analytic results. These analytic results should then be transformed to a FORTRAN code, with no need of extra labor. Under the same choice of approximations, this FORTRAN code should be similar to the one presented here, admittedly after considerable labor. In any case though, no other such $\gamma\gamma \to ZZ$ code seems to exist at present.

4 Conclusions

We have presented here the code gamgamZZ, contained in gamgamZZ.tar.gz [26]. This consists of four codes. Codes **sm1_1** and **mssm1_1** calculate the 10 basic helicity amplitudes (10) for $\gamma\gamma \to ZZ$, in SM and MSSM respectively; while codes **sm2** and **mssm2** calculate the cross sections in (12-17). When the Z polarization is not looked at, these cross sections constitute all possible observables in an $ILC_{\gamma\gamma}$.

The accompanying Readme.dat file contains all necessary instructions for compiling and running the codes [26]. The only restriction, applying to the MSSM case, is that the soft SUSY breaking parameters and μ must be real. But if interest arises, this restriction could be easily overcome, by changing certain couplings in the codes.

Since the codes **sm1_1** and **mssm1_1** determine all possible helicity amplitudes, the results should also be useful for calculating any kind of Z-polarization effects observable in $ILC_{\gamma\gamma}$, in either SM or MSSM.

Acknowledgments:
We are grateful to Fernand Renard and A. F. Zarnecki for discussions. GJG also gratefully acknowledges the support from the European Union program MRTN-CT-2004-503369.

[4]Possibly employing useful approximations, like neglecting chargino mixing in boxes, as we have done here.

References

[1] K.A. Assamagan *et.al.* , hep-ph/0406152.

[2] B.C. Allanach *et.al.* , Les Houches physics at TeV colliders 2005 beyond the standard model working group: Summary report to the Les Houches Workshop on Physics at TeV Colliders, Les Houches, France, 2-20 May 2005, hep-ph/0602198

[3] See *e.g.* A. Strumia and F. Vissani, hep-ph/0606054.

[4] E.A. Baltz, M. Battaglia, M.E. Peskin and T. Wizansky, hep-ph/0602187; K. Mönig, Int. J. Mod. Phys. **A21**:1974 (2006), hep-ph/0509159; W. Killian and P.M. Zerwas, Talk at the 2nd ILC Accelerator Workshop, Snowmass, Colorado, 14-27 Aug 2005, hep-ph/06012217.

[5] J.A. Aguilar-Saavedra *et.al.* , (SPA convention), Eur. Phys. J. **C46**:43 (2006), hep-ph/0511344; A Djouadi, M. Drees and Jean-Loic Kneur, hep-ph/0602001; A. Djouadi, hep-ph/0503173.

[6] A. Belyaev *et.al.* , heph/0609079.

[7] "TESLA Technical Design Report Part I: Executive Summary," eds. F. Richard, J. R. Schneider, D. Trines and A. Wagner, DESY, Hamburg, 2001 [hep-ph/0106314]. "TESLA Technical Design Report Part III: Physics at an e^+e^- Linear Collider," eds. R.-D. Heuer, D. Miller, F. Richard, P. M. Zerwas, DESY, Hamburg, 2001 [hep-ph/0106315].

[8] J. R. Ellis, E. Keil and G. Rolandi, "Options for Future Colliders at CERN," CERN-EP-98-03;
J. P. Delahaye *et.al.* , "CLIC—a Two-Beam Multi-TeV e^+e^- Linear Collider," in: *Proc. of the 20th Intl. Linac Conference LINAC 2000* ed. Alexander W. Chao, eConf C000821, MO201 (2000), physics/0008064;
E. Accomando *et al.* [CLIC Physics Working Group Collaboration], "Physics at the CLIC multi-TeV linear collider," CERN, Geneva, 2004, hep-ph/0412251.

[9] R.-D. Heuer, Acta Phys. Polon. **B37**:1039 (2006) .

[10] I.F. Ginzburg, G.L. Kotkin, V.G. Serbo and V.I. Telnov, Nucl. Instr. and Meth. **205**, 47 (1983); I.F. Ginzburg, G.L. Kotkin, V.G. Serbo, S.L. Panfil and V.I. Telnov, Nucl. Instr. and Meth. **219**,5 (1984); J.H. Kühn, E.Mirkes and J. Steegborn, Z. f. Phys. **C57**:615 (1993); V. Telnov, hep-ex/0003024, hep-ex/0001029, hep-ex/9802003, hep-ex/9805002, hep-ex/9908005; I.F. Ginzburg, hep-ph/9907549; R. Brinkman hep-ex/9707017; D.S. Gorbunov, V.A. Illyn, V.I. Telnov, hep-ph/0012175; "TESLA Technical Design Report, Part VI, Chapter 1: Photon Collider at TESLA", B. Badelek *et al.*, DESY, Hamburg, 2001, [hep-ex/0108012].

[11] H. Burkhardt and V. Telnov, "CLIC 3-TeV Photon Collider Option", CERN-SL-2002-013-AP.

[12] V.I. Telnov, talk at the PHOTON2005 and PLC2005 Conference, Warsaw and Kazimierz, Poland, Sep 2005, Acta Phys. Polon. **B37**:1049 (2006) , Archive: physics/0604108.

[13] M. Mühlleitner and P.M. Zerwas, Acta Phys. Polon. **B37**:1021 (2006) , hep-ph/0511339

[14] G.J. Gounaris, J. Layssac and F.M. Renard, Z. f. Phys. **C62**:139 (1994), hep-ph/9309324; M. Bailargeon, G. Belanger and F. Boudjema, Nucl. Phys. **B500**:1997 (224), hep-ph/9701372; O. Nactman, F. Nagel, M. Pospischil, Eur. Phys. J. **C45**:679 (2006), hep-ph/0508132; O. Nachtmann, F. Nagel, M. Pospischil, A. Utermann Eur. Phys. J. **C46**:93 (2006), hep-ph/0508133.

[15] O. Nachtmann, F. Nagel, M. Pospischil, A. Utermann, Eur. Phys. J. **C45**:679 (2006), hep-ph/0508132; Eur. Phys. J. **C46**:93 (2006), hep-ph/0508133.

[16] J. Sekaric, DESY-THESIS-2005-042, hep-ph/0512307; P. Nieżurawski, hep-ph/0503295.

[17] G. Jikia and A. Tkabladze, Phys. Lett. **B323**:453 (1994); M. Böhm, R. Schuster Z. f. Phys. **C63**:219 (1994).

[18] G. Jikia and A. Tkabladze, Phys. Lett. **B332**:441 (1994).

[19] G. Jikia Nucl. Phys. **B405**:24 (1993), Phys. Lett. **B298**:224 (1993).

[20] G.J. Gounaris, P.I. Porfyriadis, F.M. Renard, hep-ph/9812378, Phys. Lett. **B452**:76 (1999), Phys. Lett. **B464**:350 (1999) (E); G.J. Gounaris, P.I. Porfyriadis, F.M. Renard, hep-ph/9902230, Eur. Phys. J. **C9**:673 (1999).

[21] G.J. Gounaris, J. Layssac, P.I. Porfyriadis and F.M. Renard, hep-ph/9904450, Eur. Phys. J. **C10**:499 (1999).

[22] G.J. Gounaris, J. Layssac, P.I. Porfyriadis and F.M. Renard, Eur. Phys. J. **C13**:79 (2000), hep-ph/9909243.

[23] G.J. Gounaris, P.I. Porfyriadis and F.M. Renard, Eur. Phys. J. **C19**:57 (2001), hep-ph/0010006.

[24] G.J. Gounaris and F.M. Renard, Phys. Rev. Lett. **94**:131601 (2005), hep-ph/0501046, and the addendum in Phys. Rev. **D73**:097301 (2006), hep-ph/0604041.

[25] G. Passarino and M. Veltman Nucl. Phys. **B160**:151 (1979).

[26] All neccessary files are contained in gamgamZZ.tar.gz, which may be downloaded from http://users.auth.gr/∼gounaris/FORTRANcodes/ .

[27] M. Jacob and G.C. Wick, Annals of Phys. **7**:404 (1959).

[28] A. Djouadi, M.M. Mühlleitner and M. Spira, hep-ph/0609292; A. Djouadi, J. Kalinowski and M. Spira, HDECAY, hep-ph/9704448, Comput. Phys. Commun. **108**:56 (1998).

[29] T. Hahn, LoopTools, http://www.feynarts.de/looptools/; T. Hahn and M. Pérez-Victoria, hep-ph/9807565; G.J. van Oldenborgh and J.A.M. Vermaseren, Z. f. Phys. **C46**:425 (1990).

[30] J.M. Cornwall, D.N. Levin, and G. Tiktopoulos, Phys. Rev. **D10**:1145 (1974); M.S. Chanowitz, and M.K. Gaillard, Nucl. Phys. **B261**:379 (1985); G.J. Gounaris, R. Kögerler and H. Neufeld, Phys. Rev. **D34**:3257 (1986).

[31] A. F. Zarnecki, Acta Phys. Polon. **B34**:2741 (2003) , hep-ex/0207021.

[32] T. Hahn and M. Perez-Victoria, Comput. Phys. Commun. **118**:153 (1999); T. Hahn, hep-ph/0406288, hep-ph/0506201.

[33] B. Bélanger, F. Boudjema, J. Fujimoto, T. Ishikawa, T. Kameko, K. Kato and Y. Shimizu, hep-ph/0308080.

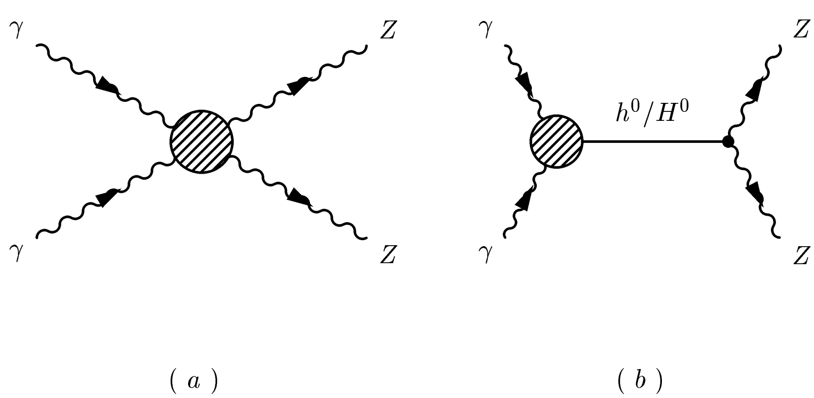

Figure 1: Feynman Diagrams for the $\gamma\gamma \to ZZ$ process in SM and MSSM models.

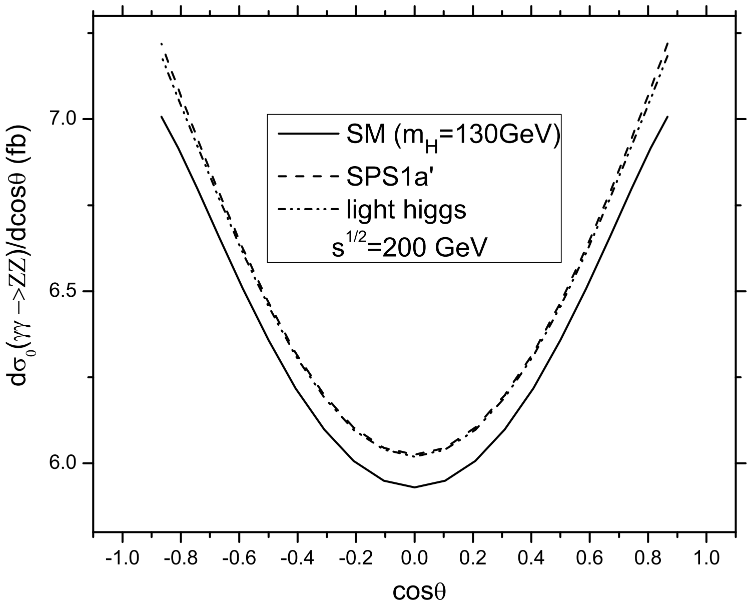

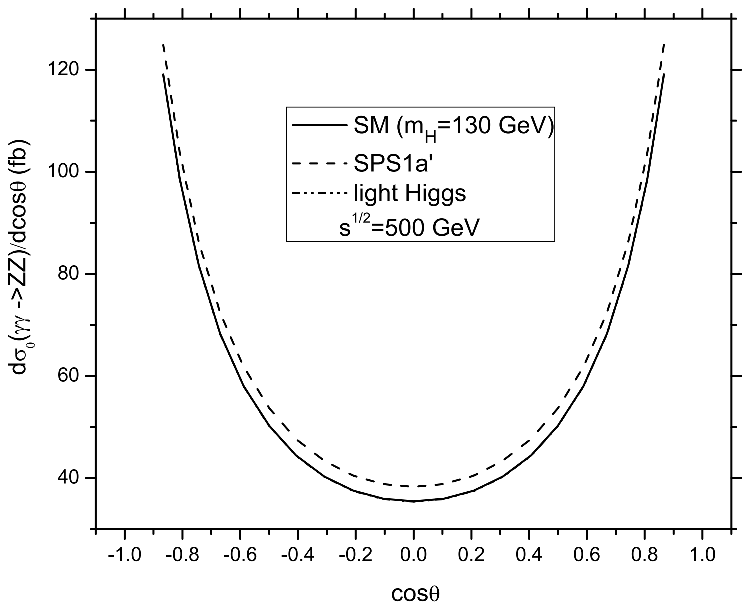

Figure 2: Differential cross section $d\sigma_0(\gamma\gamma \rightarrow ZZ)/d\cos\theta$ as a function of $\cos\theta$, in SM, $SPS1a'$ [5] and the light higgs [6] benchmark model.

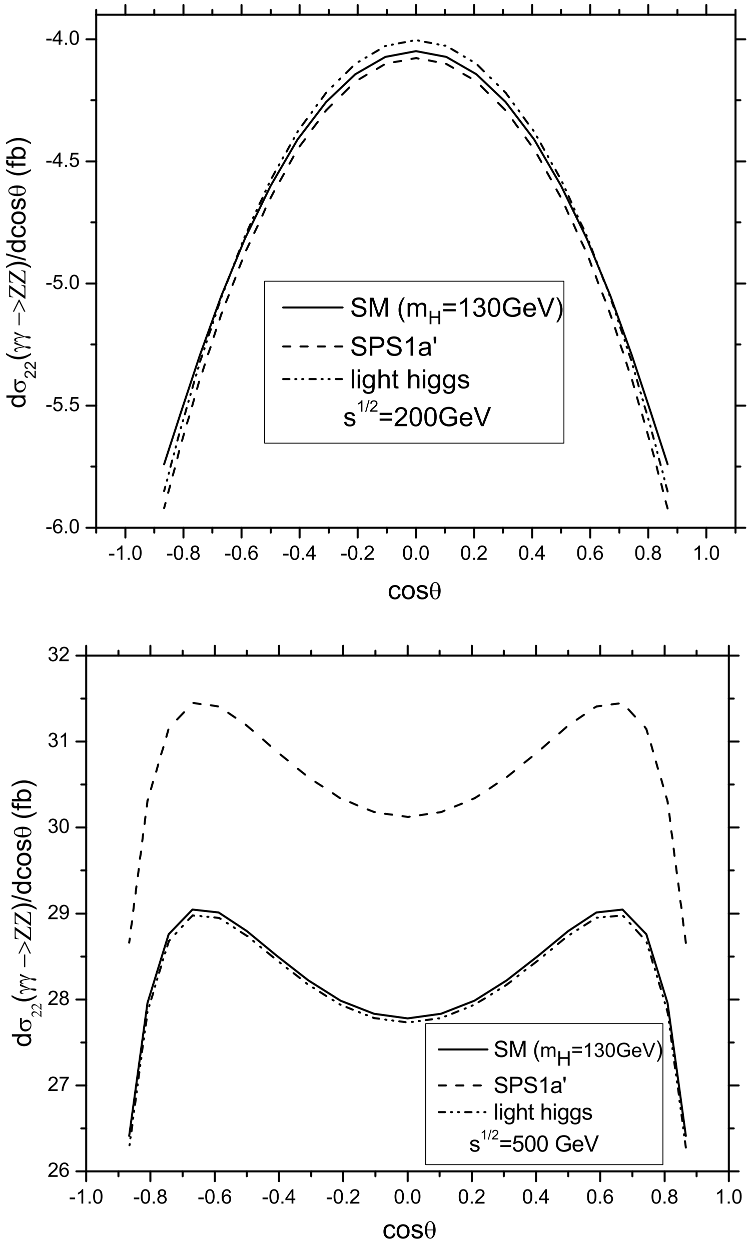

Figure 3: Differential cross section $d\sigma_{22}(\gamma\gamma \to ZZ)/d\cos\theta$ as a function of $\cos\theta$, in SM, $SPS1a'$ [5] and the light higgs [6] benchmark model.

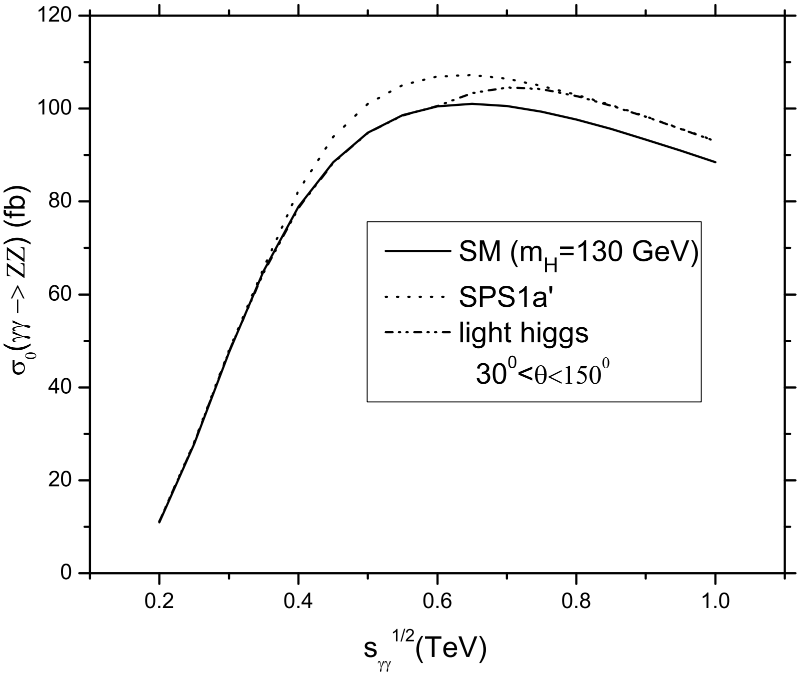

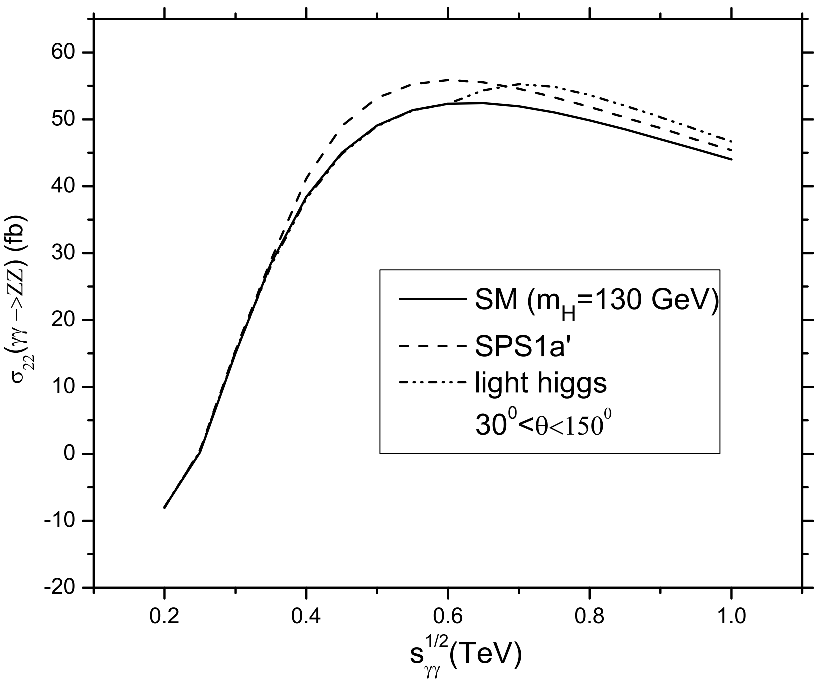

Figure 4: Integrated cross sections $\sigma_0(\gamma\gamma \to ZZ)$ and $\sigma_{22}(\gamma\gamma \to ZZ)$, as functions of the center of mass photon-photon energy $\sqrt{s} = \sqrt{s_{\gamma\gamma}}$, in SM, $SPS1a'$ [5] and the light higgs [6] benchmark model.